INTERNATIONAL JOURNAL FOR NUMERICAL METHODS IN FLUIDS
Int. J. Numer. Meth. Fluids 2005; **47**:789–801
Published online 27 January 2005 in Wiley InterScience (www.interscience.wiley.com). DOI: 10.1002/fld.858

Towards mesh adaptivity for geophysical turbulence: continuous mapping approach

Piotr K. Smolarkiewicz[1,*,†] and Joseph M. Prusa[2]

[1]*National Center for Atmospheric Research, Boulder, CO 80307, U.S.A.*
[2]*Iowa State University, Ames, IA 50011, U.S.A.*

SUMMARY

Looking forward towards mesh adaptivity for simulating turbulent atmospheric/oceanic flows, we are pursuing advanced algorithms for evaluating vector differential operators cast in time-dependent curvilinear co-ordinates. In this paper, we review our effort to date with the development of a deformable-co-ordinates multi-scale anelastic model designed from the bottom-up relying on strengths of non-oscillatory transport methods. We have shown in earlier works that effective multi-scale adaptive numerical models for high-Reynolds-number meteorological flows can be designed that dispense with rigorous evaluation of the more cumbersome of the vector differential operators, such as the curl or the strain rate. These operators are nonetheless important for budget analyses of the model results, estimating physical uncertainties, driving the mesh adaptivity itself, and extending the model's applicability beyond standard meteorological situations. Here, we discuss selected extensions of the generic explicitly inviscid approach. Copyright © 2005 John Wiley & Sons, Ltd.

KEY WORDS: geophysical turbulence; large eddy simulation; finite difference methods for fluids; mesh adaptivity

1. INTRODUCTION

The Earth's atmosphere and oceans are essentially incompressible, highly turbulent fluids. Recently [1], we summarized the efficient application of non-oscillatory forward-in-time (NFT) methods to accurately simulate a broad range of flows in these fluids. In particular, we demonstrated that NFT methods offer a means of implicit subgrid-scale (SGS) modelling that can be quite effective in assuring a quality large-eddy-simulation (LES) of high Reynolds

*Correspondence to: Piotr K. Smolarkiewicz, National Center for Atmospheric Research, Boulder, CO 80307, U.S.A.
†E-mail: smolar@ucar.edu

Contract/grant sponsor: Department of Energy

Received 27 April 2004
Revised 17 August 2004
Accepted 17 August 2004

number geophysical flows. The implicit SGS property of NFT methods[‡] is especially important where complications such as large span of scales, density stratification, planetary rotation, inhomogeneity of the lower boundary, and inhomogeneity of the numerical grid, make explicit modelling of subgrid-scale motions difficult.

Looking forward towards mesh adaptivity for simulating geophysical turbulence, we have developed a generalized mathematical framework for the implementation of deformable co-ordinates in a generic Eulerian/semi-Lagrangian NFT format [5, 6]. The key element of the framework is a time-dependent co-ordinate transformation, implemented rigorously throughout the governing equations of the non-hydrostatic anelastic model for simulating a broad range of idealized atmospheric/oceanic flows on scales from micro to planetary [1]. A computational model that is designed from the bottom-up combining NFT algorithms and generalized co-ordinates is ideally suited for continuous grid adaptation. The robust performance of NFT methods enables the ability to mimic 'nested' grids [5] and to accommodate large-amplitude undulations of the model boundaries [6]. The ability of NFT methods to supply an effective implicit SGS model facilitates LES studies in generalized co-ordinates by obviating the task of incorporating viscous stress; whereas evaluating the vorticity (in generalized co-ordinates) is not required due to the momentum/velocity formulation of the governing equations.

Although not imperative for simulating geophysical turbulence, rigorous and accurate representation of the vector differential calculus in generalized co-ordinates is important. The curl operator, $\nabla\times$, is essential for accurate evaluation of vorticity/potential-vorticity budgets—a discriminating tool for analysing complex vortical flows (see Reference [7] for an example). The strain-rate tensor, $[\nabla\mathbf{v} + \nabla\mathbf{v}^{\mathrm{T}}]$, is a key element of direct numerical simulation (DNS). Knowledge of its exact form in generalized co-ordinates allows one to extend the expertise of meteorological models to low-Reynolds-number flows, in the spirit of laboratory studies which often supplement research on the dynamics of atmospheres and oceans (e.g. References [1, 7, 8]). Also, it is a key element of explicit SGS models that are useful, beyond standard LES studies, for diagnosing SGS fluctuations and flow uncertainties. Finally, because the curl and gradient operators emphasize fundamental aspects of fluid flows, they may serve well as discriminating indicators for *driving* the grid adaptivity itself.

In this paper we review our effort to date with the development of an adaptive multi-scale anelastic model for geophysical flows, proven already useful in a generic explicitly inviscid form. In particular, we discuss the evaluation of fundamental differential operators cast in generalized time-dependent co-ordinates. Our concern is with the assurance that the resulting finite-difference formulations minimize truncation-error departures from vector differential identities, such as $\forall\phi(\mathbf{x},t)\nabla\times\nabla\phi\equiv 0$, $\forall\mathbf{A}(\mathbf{x},t)\nabla\bullet\nabla\times\mathbf{A}\equiv 0$, and that the strain and strain-rate tensors remain objective (viz. observer independent [9]). These properties (in general, of exterior derivative in the *Cartan*-algebra of differential forms [10]) are particularly important for meteorological applications. Their violations can result in spurious vorticity production at free-slip boundaries, boundary layer separations, drag in potential flows, eddy shedding in the lee of mountains, and generation of turbulence from planetary rotation, to name a few. Although the importance of respecting vector differential calculus in numerical models is widely appreciated, and the principles underlying suitable approximations are well established

[‡]For a theoretical rationale and result analysis using methods employed in this study see References [2] and [3, 4], respectively.

for centred-in-space finite-volume discretizations, the extensions to NFT methods are seldom addressed [11].

The fundamental differential operators have a tangible, physical existence that is independent of any co-ordinate-based description. However, co-ordinate-based representations are necessary for computing the explicit form of all requisite terms. Since the precise form of the terms depends upon the co-ordinate system being used, a tensor representation is preferable. The latter reveals [5] three distinct forms of velocity (physical, contravariant, and solenoidal) helpful for designing an efficient, high-Reynolds-number NFT fluid solver in generalized co-ordinates. Applications addressed here also require consideration of the covariant form. With the four distinct forms of velocity and numerous identities—which arise from the co-ordinate-invariance of geometric properties of the time-evolving physical domain—there are a number of various co-ordinate-dependent operator representations. Although they are all analytically equivalent, they lead to various numerical approximations that are not equally effective.

The paper is organized as follows. In the following section we outline the governing anelastic-model equations and summarize the computational approach. In Section 3, we discuss extensions for curvilinear representation of the vorticity, Fickian diffusion, strain, and stress. Section 4 concludes the paper with an example of a strongly stratified rapidly rotating flow past a long winding valley, an outstanding problem of mesoscale meteorology.

2. ANELASTIC FLUID MODEL IN DEFORMABLE COORDINATES

2.1. Motivation

Because of the enormous span of the spatial and temporal scales, and the wave phenomena important in geophysical fluids, explicit integrations of generic compressible equations are impractical for the majority of applications. In order to account for this broad range of scales, while deriving a numerical model still useful with existing computational resources, one has no choice but to invoke analytic or numerical approximations that allow for reasonably large time-step integrations of the governing equations. In effect, meteorological models encompass a variety of approximate (filtered) systems of fluid equations (e.g. hydrostatic, elastic, anelastic, Boussinesq, cf. Reference [12]) and engender many split-explicit or semi-implicit methods for their integration [13].

For research studies of all-scale geophysical fluids, we have found the anelastic non-hydrostatic system beneficial. The anelastic approximation may be thought of as a generalized Boussinesq approximation where the effects of density variations on mass balance and inertia are neglected in the equations of mass continuity and momentum, but are accounted for in the buoyancy forces. The classical, incompressible, Boussinesq system is applicable to shallow motions with small material displacement compared to characteristic vertical scale of the fluid, thereby allowing for a simple uniform reference state. The anelastic approximation extends this concept by accounting for the density/temperature stratification of the static background. Although the non-hydrostatic anelastic equations are known to be accurate for modelling the elements of weather and climate up to synoptic scale [14], their suitability for global weather and climate prediction has been often criticized—recently, using arguments of linear normal mode analysis [12]. Notwithstanding, our numerical results [15, 16] document that the

anelastic equations adequately capture a range of idealized planetary flows. This has important practical consequences. Inherent in the anelastic system are (i) the Boussinesq linearization of the pressure gradient forces and the mass fluxes in the momentum and mass continuity equations, respectively, and (ii) the anelasticity *per se*, equivalent to taking the limit of an infinite speed of sound. Working in concert, these two approximations greatly simplify the design of second-order accurate, flexible, and computationally efficient (viz., implicit with respect to inertia-gravity waves) research models for a broad range of geophysical flows. This is especially important within the class of NFT models, where two-time-level self-adaptive non-linear numerics lead inevitably to difficult non-linear elliptic problems for the implicit discretization of the fully compressible Euler equations. From the viewpoint of numerical engineering, the anelastic model transmutes easily into either a compressible/incompressible Boussinesq, or an incompressible Euler system [15].

2.2. *Analytic formulation*

To address a broad class of geophysical flows in a variety of domains,—with, optionally, Dirichlet, Neumann, or periodic boundaries in each direction—we formulate (and solve) the governing equations in transformed co-ordinates $(\bar{t},\bar{x},\bar{y},\bar{z})$ within a computational domain $\mathbf{S}_\mathrm{t}$ with, in general, cuboidal, toroidal, or a spheroidal topology implied by the physical boundary conditions. The co-ordinates (t,x,y,z) in the physical domain $\mathbf{S}_\mathrm{p}$ are assumed orthogonal and stationary—Cartesian or spherical are typical examples. The physical domains admitted under the homeomorphism

$$(\bar{t},\bar{x},\bar{y},\bar{z}) \equiv (t, E(t,x,y), D(t,x,y), C(t,x,y,z)) \tag{1}$$

cover a range from the canonical Cartesian box, to spherical shells with irregular undulating boundaries. In the latter case, the topology of the cuboid is still an option. By removing an arbitrary small circle about the poles, the traditional differentiation across the pole is replaced with Neumann boundaries on the circle, thereby simplifying the use of the same model for both global and small-to-mesoscale applications. This option is important for improving communications in the massively parallel variant of the model code when a grid deforms in the vicinity of the poles. The assumption in (1) that the transformed horizontal co-ordinates $(\bar{x},\bar{y})$ are independent of the vertical co-ordinate z follows the primary hydrostatic structure of the atmosphere and oceans and simplifies the metric terms. Examples of mappings embedded in (1) include the classical terrain-following co-ordinates of Gal-Chen and Somerville [17], their time-dependent extensions [6, 18], as well as a horizontal stretching whereby the horizontal co-ordinates in $\mathbf{S}_\mathrm{t}$ are arbitrary (in theory subject to C^2 continuity; cf. Reference [5]) functions of the time and horizontal co-ordinates in $\mathbf{S}_\mathrm{p}$.

Given transformation (1), the anelastic equations of Lipps and Hemler [19] can be written as follows

$$\frac{\partial(\rho^* \overline{v}^{sk})}{\partial \bar{x}^k} = 0 \tag{2}$$

$$\frac{\mathrm{d}v^j}{\mathrm{d}\bar{t}} = -\widetilde{G}^k_j \frac{\partial \pi'}{\partial \bar{x}^k} + g\frac{\theta'}{\theta_\mathrm{b}}\delta_3{}^j + \mathscr{F}^j + \mathscr{V}^j \tag{3}$$

$$\frac{\mathrm{d}\theta'}{\mathrm{d}\bar{t}} = -\overline{v}^{sk}\frac{\partial \theta_\mathrm{e}}{\partial \bar{x}^k} + \mathscr{H} \tag{4}$$

where the physical and geometrical aspects intertwine each other. Insofar as the physics is concerned v^j denotes components of the *physical velocity* (defined in $\mathbf{S}_\mathrm{p}$);[§] θ, ρ, and π denote potential temperature, density, and a density-normalized pressure; g is the acceleration of gravity; $\mathscr{F}^j$ symbolizes the deviation of inertial forces (e.g. Coriolis and geospherical metric accelerations) from the geostrophically balanced ambient (or environmental) state v_e^j, θ_e; whereas $\mathscr{V}^j$ and $\mathscr{H}$ symbolize viscous dissipation of momentum and diffusion of heat, respectively. Primes denote perturbations with respect to the environmental state, and the subscript $_\mathrm{b}$ refers to the basic state, i.e. a horizontally homogeneous hydrostatic reference state of a Boussinesq type expansion around a constant stability profile (cf. Section 2b in Reference [20], for a discussion).

The geometry of the co-ordinates in (1) enters the governing equations as follows: $\rho^* := \rho_\mathrm{b}\,\overline{G}$,[¶] $\overline{G}$ denoting the Jacobian of the transformation (defined in the subsequent paragraph), and $j,k = 1,2,3$ correspond to 'x', 'y', 'z' components, respectively, in either $\mathbf{S}_\mathrm{p}$ or $\mathbf{S}_\mathrm{t}$. In the momentum equation (3), $\widetilde{G}_j^k := \sqrt{g^{jj}}\ (\partial\overline{x}^k/\partial x^j)$ are renormalized elements of the Jacobi matrix where summation is not implied over j, and δ_3^j is the Kronecker delta. The coefficients g^{jj} are the diagonal elements of the conjugate metric tensor of $\mathbf{S}_\mathrm{p}$ (defined below). The total derivative is given by $\mathrm{d}/\mathrm{d}\overline{t} = \partial/\partial\overline{t} + \overline{v^*}^k(\partial/\partial\overline{x}^k)$, where $\overline{v^*}^k := \mathrm{d}\overline{x}^k/\mathrm{d}\overline{t} := \dot{\overline{x}}^k$ is the *contravariant velocity*. Appearing in continuity (2) and potential temperature (4) equations is the *solenoidal velocity* (so named for distinction, because of the form continuity takes with it)

$$\overline{v^s}^k := \overline{v^*}^k - \frac{\partial\overline{x}^k}{\partial t} \tag{5}$$

that readily follows—given $\rho_\mathrm{b} = \rho_\mathrm{b}(\mathbf{x})$, and the time-independent co-ordinate system in $\mathbf{S}_\mathrm{p}$—from the tensor invariant form of anelastic continuity $\overline{G}^{-1}\partial(\rho_\mathrm{b}\overline{G}\,\overline{v^*}^i)/\partial\overline{x}^i \equiv 0$, where $i = 0,1,2,3$ ($i = 0$ refers to time $\overline{t}$); see Reference [5] and the references therein for a discussion. Use of the solenoidal velocity facilitates the solution procedures because it preserves the incompressible character of numerical equations. While numerous relationships can be derived that express any velocity (solenoidal, contravariant, or physical) in terms of the other, in either transformed or physical co-ordinate system [5], a particularly useful transformation

$$\overline{v^s}^j = \widetilde{G}_k^j v^k \tag{6}$$

relates the solenoidal and physical velocities directly.

The elements of the metric tensor of the transformed co-ordinates are $\overline{g}_{mn} = g_{pq}(\partial x^p/\partial\overline{x}^m)(\partial x^q/\partial\overline{x}^n)$, where g_{pq} denotes the metric tensor of the physical co-ordinate system (which need not be Cartesian). The Jacobian is then $\overline{G} = |\overline{g}_{mn}|^{1/2}$. The elements of g_{pq} may be computed from the definition of the fundamental metric $\mathrm{d}s^2 = g_{pq}\mathrm{d}x^p\mathrm{d}x^q$ and the linear system $g_{pk}g^{kq} \equiv \delta_p^q$. Employing $g_{pq} = 0$ for $p \neq q$—a consequence of the assumed orthogonality of the co-ordinates in $\mathbf{S}_\mathrm{p}$—the elements of the conjugate metric tensor, needed in (3), are

[§]In meteorological applications, the physical velocity is typically defined using a local Cartesian system and so has dimensions of length/time; a distinct representation of the physical velocity, $\overline{v}^j \neq v^j$, also exists for the transformed co-ordinate system; cf. Reference [5].

[¶]We use := to mean *defined as*, to distinguish from ≡ (*identically*).

computed from $g^{jj} = 1/g_{jj}$. Note that unlike g^{pq}, the metric coefficients $\widetilde{G}_p^q$ appearing in Equations (3) and (6) are *not* symmetric (i.e. $\widetilde{G}_p^q \neq \widetilde{G}_q^p$).

2.3. Numerical approximations

Given (2), each prognostic equation of the anelastic system (3) and (4) can be written compactly either as a Lagrangian evolution equation

$$\frac{\mathrm{d}\psi}{\mathrm{d}\bar{t}} = R \tag{7}$$

or an Eulerian conservation law

$$\frac{\partial \rho^* \psi}{\partial \bar{t}} + \overline{\nabla} \bullet (\rho^* \overline{\mathbf{v}}^* \psi) = \rho^* R \tag{8}$$

Here ψ symbolizes v^j or θ', R denotes the associated rhs, and $\overline{\nabla} \bullet := (\partial/\partial\bar{x}, \partial/\partial\bar{y}, \partial/\partial\bar{z})\bullet$.

The theory and performance of our NFT approach have been broadly documented in the literature; see Reference [1] for a succint review. In essence, we approximate either (8) or (7) to second-order accuracy in space and time, employing a formal congruency of the Eulerian [21] and semi-Lagrangian [22] optional model algorithms, respectively. In effect, either algorithm can be written in the compact form

$$\psi_{\mathbf{i}}^{n+1} = \mathrm{LE}_{\mathbf{i}}(\widetilde{\psi}) + 0.5\Delta t R_{\mathbf{i}}^{n+1} \tag{9}$$

where $\psi_{\mathbf{i}}^{n+1}$ is the solution sought at the grid point $(\bar{t}^{n+1}, \overline{\mathbf{x}}_{\mathbf{i}})$, $\widetilde{\psi} := \psi^n + 0.5\Delta t R^n$, and LE denotes a two-time-level either advective semi-Lagrangian or flux-form Eulerian NFT transport operator. In the Eulerian scheme, LE integrates the homogeneous transport equation (8), i.e. LE advects $\widetilde{\psi}$ using a fully second-order accurate multidimensional NFT advection scheme [1, 23]; whereas in the semi-Lagrangian algorithm, LE remaps transported fields, which arrive at the grid points $(\bar{t}, \overline{\mathbf{x}}_{\mathbf{i}})$, back to the departure points of the flow trajectories $(\bar{t}^n, \overline{\mathbf{x}}_o(\bar{t}^{n+1}, \overline{\mathbf{x}}_{\mathbf{i}}))$ also using NFT advection schemes [22, 24].

For inviscid adiabatic flows, Equation (9) represents a system of equations that is implicit with respect to all dependent variables in (3) and (4), since forcing terms are assumed to be unknown at $n+1$. This system is inverted algebraically to construct expressions for the solenoidal velocity components that are subsequently substituted into (2) to produce an elliptic equation for pressure (see Reference [5] for the complete development). The elliptic pressure equation is solved, subject to appropriate boundary conditions [5, 6], using a preconditioned non-symmetric Krylov-subspace solver [25]. Given the updated pressure, and hence the updated solenoidal velocity, the updated physical and contravariant velocity components are constructed from the solenoidal velocities using transformations (6) and (5), respectively. Non-linear terms in R^{n+1} (e.g. metric terms arising on the globe) may require outer iteration of the system of equations generated by (9) [15]. When included, diabatic, viscous, and subgrid-scale forcings may be first-order accurate and explicit, e.g. assume $\mathrm{SGS}(\psi^{n+1}) = \mathrm{SGS}(\psi^n) + \mathcal{O}(\Delta t)$ in R^{n+1}, see Section 3.5.4 in Reference [23]. For extensions to moist processes, see Reference [16].

3. EXTENSIONS: CURVILINEAR OPERATOR CALCULUS

3.1. Tensor identities

Developments in this paper make use of several tensor identities. For the reader's convenience, here, we highlight two of them that we have found particularly useful both for manipulating analytic tensor fields into forms preferred in the numerical model and for evaluating transformation coefficients in the model code.‖

The first identity, although elementary, has profound implications for the implementation of the operator calculus in the numerical model. In a four-dimensional space, it consists of 16 simultaneous equations (differential identities) that relate the elements of the Jacobi and inverse Jacobi matrices of the transformation defining $\mathbf{S}_t$

$$\delta_s^r \equiv \frac{\partial \overline{x}^r}{\partial x^q}\frac{\partial x^q}{\partial \overline{x}^s} \tag{10}$$

Given our specified functional form for the transformation, (1), 6 of these reduce to trivial statements (i.e. $0=0$ or $1=1$), leaving 10 equations relating 20 metric coefficients. Since in our model the problem is solved in $\mathbf{S}_t$, the physical co-ordinates of $\mathbf{S}_p$ are treated as dependent variables, that is, $x^q = x^q(\overline{x}^r)$. Once the $\partial x^q/\partial \overline{x}^s$ have been determined (either analytically or numerically), the simultaneous equations (10) are used to determine the inverse metric coefficients $\partial \overline{x}^r/\partial x^q$. The use of these differential identities is important for ensuring conservative properties of the numerical model. The latter becomes exposed in the proof (not shown) of the second identity

$$\frac{G}{\overline{G}}\frac{\partial}{\partial \overline{x}^r}\left(\frac{\overline{G}\partial \overline{x}^r}{G\partial x^s}\right) \equiv 0 \tag{11}$$

termed the geometric conservation law, or GCL.** The left-hand side can be recognized as the divergence in $\mathbf{S}_t$ of the contravariant form $(1/G)\partial \overline{x}^r/\partial x^s$ multiplied by the Jacobian of $\mathbf{S}_p$. This form gives weighted 'velocities' ($s=0$), or 'stretching factors' ($s=1,2,3$) between $\mathbf{S}_p$ and $\mathbf{S}_t$. Evidently, (11) is a set of four statements about the *conservation of space*. Various components of the GCL have been recognized as being of fundamental importance in numerical models for curvilinear co-ordinates for 25 years [26]. The generalized GCL in (11) arises naturally from the co-ordinate invariance of conservation equations written in tensor form, and the use of the differential identities (10) is important for satisfying the GCL.

3.2. Vorticity

The physical definition of vorticity, $\boldsymbol{\omega} = \nabla \times \mathbf{v}$, is independent of the choice of co-ordinate system that one uses to describe a fluid flow. In curvilinear co-ordinates, however, one needs to carefully distinguish between covariant and contravariant (as well as mixed) forms in order that a *physical* vorticity with *appropriate* dimensions may be recovered, for this is what we would observe in a laboratory or in the field.

‖For examples, see discussion surrounding Equation (13) in Reference [6].

**This version of GCL has been used to derive (2) from the tensor invariant anelastic continuity equation; cf. discussion following (5).

Following the notation of the preceding section, we begin with the formal definition of vorticity in the co-ordinate-invariant covariant tensor form, cf. Reference [27]:

$$\overline{\omega^*}_{jk} = \overline{v^*}_{k,j} - \overline{v^*}_{j,k} \tag{12}$$

Here, $\overline{v^*}_j$ denotes the covariant velocity distinguished from the contravariant velocity $\overline{v^*}^j$ only by the index position,[††] and indices following a comma refer to covariant differentiation; i.e. evaluating elements of the gradient operator. In particular, for the covariant velocity

$$\overline{v^*}_{j,k} = \frac{\partial \overline{v^*}_j}{\partial \overline{x}^k} - \overline{\left\{ \begin{matrix} p \\ jk \end{matrix} \right\}} \overline{v^*}_p \tag{13}$$

The term in brackets is a Christoffel symbol of the second kind [27], and it appears due to the twisting and turning of the curvilinear co-ordinates. Similar to j,k, the index $p = 1,2,3$ corresponds to 'x', 'y', and 'z'. Because $\overline{\omega^*}_{jk}$ is skew symmetric, any three independent elements suffice to describe the vorticity *vector*.

The covariant vorticity (12) is the principal form. However, we wish to develop the physical vorticity form as a function of physical velocity gradients. In general, covariant velocities are unavailable in the model, because they are not required to solve the governing equations. Routinely stored are the physical velocity components v^j expressed in terms of the co-ordinates $\overline{\mathbf{x}}$ of the transformed space $\mathbf{S}_\mathrm{t}$ where the computation is done. In order to compute in $\mathbf{S}_\mathrm{t}$ the physical vorticity defined in $\mathbf{S}_\mathrm{p}$ in terms of v^j we: (i) write (12) for the reference system $\mathbf{S}_\mathrm{p}$ using the covariant velocities of the reference system v^*_j; (ii) rewrite the covariant velocities in terms of the physical velocities; (iii) transform all spatial derivatives into the curvilinear space $\mathbf{S}_\mathrm{t}$; and (iv) extract the physical vorticity from (12). The final result is

$$\omega^q = \varepsilon_{qjk} \sqrt{g^{kk}} \widetilde{G}^p_j \frac{\partial \sqrt{g_{kk}} v^k}{\partial \overline{x}^p} \tag{14}$$

where ε_{qjk} is the permutation symbol, and $q = 1,2,3$. The relative simplicity of expression (14) depends on the assumption of orthogonality of $(t, \mathbf{x})$ co-ordinates in $\mathbf{S}_\mathrm{p}$, see Section 2.

In order to illustrate (14) at work, we consider the numerical simulation, presented in [6], of a flow of an ideal 3D homogeneous Boussinesq fluid past oscillating membranes. The membranes form impermeable free-slip upper and lower boundaries, and their shape is prescribed, respectively, as

$$z_s(r(x,y),t) = \begin{cases} z_{s0} \cos^2(\pi r/2L) \sin(2\pi t/T) & \text{if } r/L \leqslant 1 \\ 0 & \text{otherwise} \end{cases} \tag{15}$$

$$H(x,y,t) = H_0 - z_s(x,y,t)$$

with $r = \sqrt{x^2 + y^2}$, oscillation period $T = 48\Delta t$, amplitude $z_{s0} = 51.2\Delta z$, the membranes' half-width $L = 51.2\Delta x$, where $\Delta x = \Delta y = \Delta z$, and $C(t,x,y,z) = H_0(z - z_s)/(H - z_s)$ in (1). The computational domain consists of $160 \times 160 \times 128$ grid intervals, in the horizontal and vertical, respectively, and the *LE* operator in (9) is semi-Lagrangian. The domain deformation is

[††] In any co-ordinate system, $\overline{v^*}_k = \overline{g}_{jk} \overline{v^*}^j$.

Table I. Vorticity errors in a potential flow simulation.

Field	Max |.|	Average	Standard deviation
$\Delta t\omega^1$	6.99×10^{-2}	-4.87×10^{-18}	1.90×10^{-3}
$\Delta t\omega^2$	6.98×10^{-2}	-3.19×10^{-17}	1.90×10^{-3}
$\Delta t\omega^3$	7.62×10^{-3}	2.20×10^{-18}	1.71×10^{-4}
$\Delta t\nabla \bullet \boldsymbol{\omega}^s$	2.94×10^{-5}	-7.52×10^{-18}	3.75×10^{-7}

significant, since at $t = T/4$, the upper and lower boundaries are separated merely by one-fifth of the vertical extent of the model. The magnitude of the induced flow and its variation is approximately 5 and 0.5, respectively, as measured by $\mathscr{C} \equiv \|\Delta t\overline{\mathbf{v}}^*/\Delta\overline{\mathbf{x}}\|$ and $\mathscr{L} \equiv \|\Delta t\partial\overline{\mathbf{v}}^*/\partial\overline{\mathbf{x}}\|$—the (maximal) Courant and 'Lipschitz' numbers (cf. Reference [22] for a discussion). For a graphic illustration of the simulated flow we refer the interested reader to Figure 1 in Reference [6].

Lacking diabatic forces, boundary friction, and buoyancy, the experimental set-up implies a potential-flow solution with zero integral pressure force on the bounding walls (D'Alembert paradox, cf. Reference [28]). Indeed, the authors have verified in Reference [6] that the pressure drag is on the order of round-off errors. We have computed $\boldsymbol{\omega}\Delta t$ as implied by (14), using standard centred finite-difference approximations. Since the simulated flow is clearly potential, the residual vorticity is primarily due to the truncation error of evaluating (14) itself. In general, we find the domain averaged residual vorticity($\times\Delta t$) on the order of round-off errors, with standard deviations $\lesssim 2 \times 10^{-3}$—i.e. 3 and 2 orders smaller than the flow magnitude as measured, respectively, by $\mathscr{C}$ and $\mathscr{L}$. Furthermore, divergence of the solenoidal vorticity, evaluated from the physical vorticity by means of transformation (6), is 7 and 6 orders smaller than $\mathscr{C}$ and $\mathscr{L}$. For illustration, Table I shows statistics from $t = T/4$ when the displacement of membranes is maximal but flow weak ($\mathscr{C} = 1.2$ and $\mathscr{L} = 0.14$) thereby representing the worst-case scenario.

3.3. Scalar diffusion

The diffusion of heat, symbolized by the $\mathscr{H}$ term on the rhs of (4), is a realization of the general problem for scalar diffusion. It is defined in $\mathbf{S}_\mathrm{p}$ as a divergence of the Fickian flux of the scalar field θ'. Starting with a pure covariant form of the flux $\sim \theta'_{,j}$, after suitable tensor algebra we arrive at

$$\mathscr{H} = \frac{1}{\rho^*}\frac{\partial}{\partial\overline{x}^j}\left(\alpha\rho^*\overline{g}^{jk}\frac{\partial\theta'}{\partial\overline{x}^k}\right) \tag{16}$$

expressed solely in $\mathbf{S}_\mathrm{t}$. Here, α denotes the diffusivity coefficient with the dimension of length$^2 \times$ time^{-1}.

3.4. Momentum dissipation

Our use of a curvilinear, though orthogonal and stationary, reference space represents a significant departure from earlier transformation methods discussed in the literature of computational meteorology (e.g. Reference [17]) where all relevant formulae were derived assuming Cartesian $\mathbf{S}_\mathrm{p}$. Although this approach—merely optional for Euclidean spaces—greatly

simplifies designing all-scale models for geophysical flows, it does require rederivation of all relevant formulae. This is particularly tedious for the $\mathscr{V}^j$ term on the rhs of (3). In the interest of saving journal space, here, we only highlight the chain of thoughts that lead us to the final expression for the viscous stress divergence employed in the model, additional details may be found in Reference [29].

The derivation of the viscous stress starts with the development of the strain rate tensor. Forthcoming from geometric principles, we begin by defining the strain rate tensor, $\bar{\varepsilon}_{jk}$, in terms of the time rate of change of distance elements when co-moving with the flow. Then, from the definition of the fundamental metric (see the paragraph following Equation (6)) we arrive, after some algebra, at the covariant form of the strain rate tensor

$$\overline{\varepsilon^*}_{jk} \equiv \tfrac{1}{2}(\overline{v^*}_{k,j} + \overline{v^*}_{j,k}) \tag{17}$$

the symmetric complement of the *rotation* (viz, half of the vorticity in Equation (12)) to the gradient of the covariant velocity. These are the forms which exhibit the objectivity alluded to in the introduction. In order to compute the covariant strain rate components, (17) is (i) written for $\mathbf{S}_\mathrm{p}$, (ii) (13) is used to expand the covariant derivatives, (iii) the covariant velocities are rescaled into the physical velocities, and (iv) the chain rule is used to rewrite the derivatives in terms of $\mathbf{S}_\mathrm{t}$. The final result is

$$\varepsilon^*_{jk} \equiv \frac{1}{2}\left(\sqrt{g_{kk}}\widetilde{G}^p_k \frac{\partial\sqrt{g_{jj}}v^j}{\partial\overline{x}^p} + \sqrt{g_{jj}}\widetilde{G}^q_j \frac{\partial\sqrt{g_{kk}}v^k}{\partial\overline{x}^q}\right) - \sqrt{g_{mm}}\left\{\begin{matrix} m \\ jk \end{matrix}\right\} v^m \tag{18}$$

If needed, this expression may be rescaled to yield the physical strain rate, $\varepsilon^{jk} \equiv \sqrt{g^{jj}g^{kk}}\varepsilon^*_{jk}$. Except for the Christoffel terms (which do not cancel in this case), the physical strain rate strongly parallels the form for physical vorticity (14).

Next we define the deviatoric (or viscous) stress in $\mathbf{S}_\mathrm{p}$

$$\rho_\mathrm{b}\tau^{*j}_k := 2\mu\varepsilon^{*j}_k + \lambda v^{*m}_{,m}\delta^j_k \tag{19}$$

where the two coefficients are the molecular viscosity μ and the bulk viscosity λ;[‡‡] the mixed strain rate tensor ε^{*j}_k may be generated by raising an index on the covariant form given in (18), and $v^{*m}_{,m} = -\overline{v^s}^m\partial\,\ln(\rho^*)/\partial\overline{x}^m$ from (2).

The viscous force $\mathscr{V}^j$ on the rhs of (3) consists of components of the divergence of the viscous stress tensor. After suitable tensor algebra we arrive at

$$\mathscr{V}^j = \frac{1}{\rho^*}\frac{\partial}{\partial\overline{x}^p}\left(\rho^*\widetilde{G}^p_k\sqrt{g_{jj}g_{kk}}\tau^{*\,jk}\right) - \tau^{*\,jk}\frac{\partial\sqrt{g_{jj}}}{\partial x^k} + \sqrt{g_{jj}}\left\{\begin{matrix} j \\ lm \end{matrix}\right\}\tau^{*\,lm} \tag{20}$$

with

$$\tau^{*\,jk} = 2\nu g^{jj}g^{kk}\varepsilon^*_{jk} + \kappa g^{jk}v^{*m}_{,m} \tag{21}$$

where $\nu := \mu/\rho$ is the kinematic viscosity and $\kappa := \lambda/\rho$ is the density normalized bulk viscosity. The last two terms on the rhs of (20) vanish in Cartesian $\mathbf{S}_\mathrm{p}$; the first of them arises because we use a hybrid form of the momentum equation that uses the physical velocity rather than the contravariant velocity, whereas the second reflects the intrinsic curvilinear nature of $\mathbf{S}_\mathrm{p}$.

[‡‡] We assume a Newtonian fluid and employ the traditional Stokes hypothesis.

4. EXAMPLE

In Reference [5] we addressed the mesh-refinement aspects of our curvilinear mapping approach, whereas in Reference [6] we focused on the adaptivity to variable vertical boundaries. Here, we emphasize yet another aspect, i.e. the ability to accommodate complex horizontal boundaries. To illustrate the potential of the advocated approach as a discovery tool in the area of complex geophysical flows, we highlight the original simulation of an idealized stratified rotating flow past a long winding valley. The Froude and Rossby numbers—respective measures of the relative importance of the inertial to buoyancy and Coriolis accelerations—are both about 0.6, thereby indicating significant non-linearity of the simulated flow. In spite of the relevance to weather conditions in densely populated areas, this is a poorly understood and unexplored problem—primarily, we believe, because of the lack of adequate mathematical tools. The horizontal model domain in $\mathbf{S}_\mathrm{p}$ is bounded by two sinusoids of the same x-wavelength $L_x = 400$ km, separated by constant increment 200 km in y. A cosine-shaped valley with the depth and half-width 0.8 and 30 km, respectively, is centred in the model domain. The vertical domain is 9 km deep. The ambient wind is $(U, 0, 0)$ with $U = 5$ m/s, and the buoyancy frequency $N = 0.012\ \mathrm{s}^{-1}$ and relative humidity 92% are assumed (for a discussion of moist thermodynamics and its numerical representation, see Reference [16] and references therein). Boundary conditions are periodic in both horizontal directions. Lower boundary assumes partial slip with typical (for mesoscale simulations) drag coefficient $C_d = 10^{-3}$, and the uniform normal heat flux $H_o = -0.01\ \mathrm{K\ ms}^{-1}$. The boundary-sink of heat and momentum is felt in the vertical via an arbitrarily specified 'eddy viscosity'. Its surface value $\nu = \alpha = 0.25\Delta z^2/\Delta t$ is attenuated exponentially to zero with e-folding scale $2\Delta z$. The transformed model domain

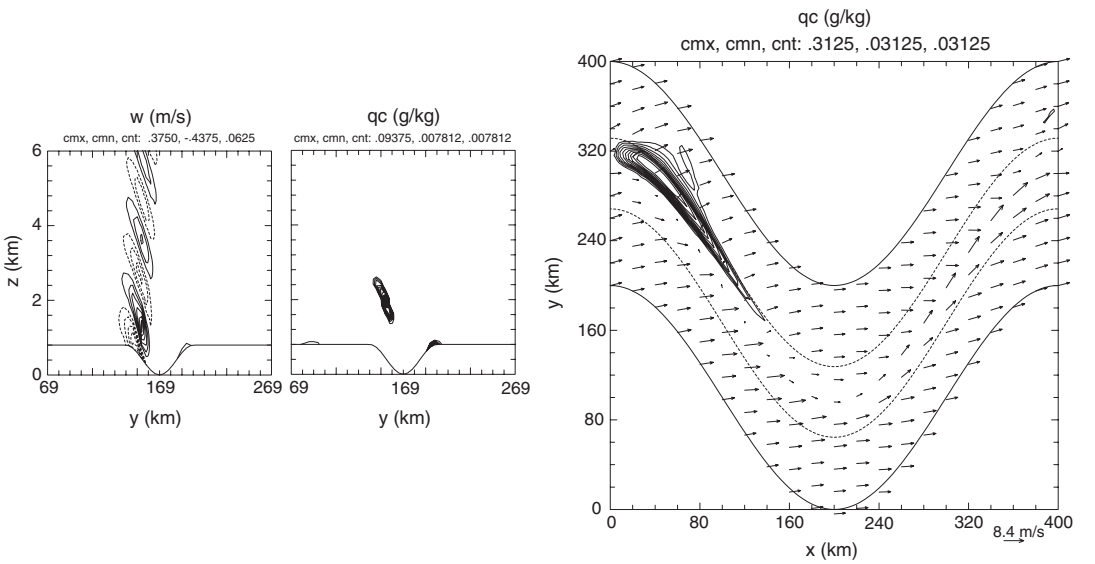

Figure 1. Vertical velocity (outer left panel) and cloud water mixing ratio (inner left panel) in the yz cross section at $x = 120$ km and cloud–water mixing ratio at bottom surface of the model (right panel); two dotted lines along the center of the sinusoidal domain outline the extent of the valley.

$\mathbf{S}_t$ is covered with $100 \times 50 \times 60$ grid increments. The simulation covers 8 h of physical time with $\Delta t = 60$ s. Figure 1 displays the solution after 8 h. The results obtained have been verified against linear estimations, and corresponding 3D/2D simulations on rectangular domains. The benefits of the advocated approach are obvious: the narrower the winding valley, the more prohibitive the cost of standard simulations on rectangular domains. Here, the gain is about a factor of 2.

ACKNOWLEDGEMENTS

This work was supported in part by the Department of Energy 'Climate Change Prediction Program' (CCPP) research initiative. The comments of the editor and two anonymous referees helped to improve the presentation.

REFERENCES

1. Smolarkiewicz PK, Prusa JM. Forward-in-time differencing for fluids: simulation of geophysical turbulence. In *Turbulent Flow Computation*, Drikakis D, Guertz BJ (eds). Kluwer Academic Publishers: Dordrecht, 2002; 207–240.
2. Margolin LG, Rider WJ. A rationale for implicit turbulence modeling. *International Journal for Numerical Methods in Fluids* 2002; **39**:821–841.
3. Margolin LG, Smolarkiewicz PK, Wyszogrodzki AA. Implicit turbulence modelling for high Reynolds number flows. *Journal of Fluids Engineering* 2002; **124**:862–867.
4. Domaradzki JA, Xiao Z, Smolarkiewicz PK. Effective eddy viscosities in implicit large eddy simulations of turbulent flows. *Physics of Fluids* 2003; **15**:3890–3893.
5. Prusa JM, Smolarkiewicz PK. An all-scale anelastic model for geophysical flows: dynamic grid deformation. *Journal of Computational Physics* 2003; **190**:601–622.
6. Wedi NP, Smolarkiewicz PK. Extending Gal–Chen and Somerville terrain-following coordinate transformation on time–dependent curvilinear boundaries. *Journal of Computational Physics* 2004; **193**:1–20.
7. Rotunno R, Grubišić V, Smolarkiewicz PK. Vorticity and potential vorticity in mountain wakes. *Journal of the Atmospheric Sciences* 1999; **56**:2796–2810.
8. Wedi NP, Smolarkiewicz PK. Laboratory for internal gravity-wave dynamics: the numerical equivalent to the quasi-biennial oscillation (QBO) analogue. *International Journal for Numerical Methods in Fluids* 2004, *ibid.*
9. Ogden RW. *Non-Linear Elastic Deformations*. Wiley: New York, 1984; 532.
10. Maurin K. *Analysis Part II*: *Integration*, *Distributions*, *Holomorphic Functions*, *Tensor and Harmonic Analysis*. Reidel Publishing Co: Dordrecht, 1980.
11. Margolin LG, Shaskhov M, Smolarkiewicz PK. A discrete operator calculus for finite difference approximations. *Computer Methods in Applied Mechanics and Engineering* 2000; **187**:365–383.
12. Davis T, Staniforth A, Wood N, Thuburn J. Validity of anelastic and other equation sets as inferred from normal-mode analysis. *Quarterly Journal of the Royal Meteorological Society* 2003; **129**:2761–2775.
13. Durran DR. *Numerical Methods for Wave Equations in Geophysical Fluid Dynamics*. Springer: Berlin, 1999.
14. Polavarapu SM, Peltier WR. The structure and nonlinear evolution of synoptic scale cyclones: life cycle simulations with a cloud-scale model. *Journal of the Atmospheric Sciences* 1990; **47**:2645–2673.
15. Smolarkiewicz PK, Margolin LG, Wyszogrodzki AA. A class of nonhydrostatic global models. *Journal of the Atmospheric Sciences* 2001; **58**:349–364.
16. Grabowski WW, Smolarkiewicz PK. A multiscale anelastic model for meteorological research. *Monthly Weather Review* 2002; **130**:939–956.
17. Gal-Chen T, Somerville CJ. On the use of a coordinate transformation for the solution of the Navier–Stokes equations. *Journal of Computational Physics* 1975; **17**:209–228.
18. Prusa JM, Smolarkiewicz PK, Garcia RR. On the propagation and breaking at high altitudes of gravity waves excited by tropospheric forcing. *Journal of the Atmospheric Sciences* 1996; **53**:2186–2216.
19. Lipps FB, Hemler RS. A scale analysis of deep moist convection and some related numerical calculations. *Journal of the Atmospheric Sciences* 1982; **39**:2192–2210.
20. Clark TL, Farley RD. Severe downslope windstorm calculations in two and three spatial dimensions using anelastic interactive grid nesting: a possible mechanism for gustiness. *Journal of the Atmospheric Sciences* 1984; **41**:329–350.
21. Smolarkiewicz PK, Margolin LG. On forward-in-time differencing for fluids: extension to a curvilinear framework. *Monthly Weather Review* 1993; **121**:1847–1859.

22. Smolarkiewicz PK, Pudykiewicz JA. A class of semi-Lagrangian approximations for fluids. *Journal of the Atmospheric Sciences* 1992; **49**:2082–2096.
23. Smolarkiewicz PK, Margolin LG. MPDATA: a finite difference solver for geophysical flows. *Journal of Computational Physics* 1998; **140**:459–480.
24. Smolarkiewicz PK, Grell GA. A class of monotone interpolation schemes. *Journal of Computational Physics* 1992; **101**:431–440.
25. Smolarkiewicz PK, Margolin LG. Variational methods for elliptic problems in fluid models. *Proceedings of the ECMWF Workshop on Developments in Numerical Methods for Very High Resolution Global Models*, 5–7 June 2000, ECMWF, Reading, U.K., 137–159.
26. Thomas PD, Lombard CK. Geometric conservation law and its application to flow computations on moving grids. *AIAA Journal* 1979; **17**:1030–1037.
27. Synge JL, Schild A. *Tensor Calculus*. Dover Press: New York, 1978.
28. Milne-Thomson LM. *Theoretical Hydrodynamics* (5th edn). The MacMillan Press Ltd.: New York, 1968.
29. Prusa JM, Smolarkiewicz PK. Dynamic grid deformation: continuous mapping approach. *Proceedings of the ECMWF Seminar on Recent Developments in Numerical Methods for Atmospheric and Ocean Modelling*, 6–10 September 2004, ECMWF, Reading, U.K., 267–283.

